The Efficient Computation of Periodic States of Cyclically Operated Chemical Processes

T. L. van Noorden[1,3], S. M. Verduyn Lunel*[2] and A. Bliek[3]

[1] *Vrije Universiteit Amsterdam, Department of Mathematics, De Boelelaan 1081A, 1081 HV Amsterdam, The Netherlands*

[2] *Universiteit Leiden, Department of Mathematics, Niels Bohrweg 1, 2333 CA Leiden, The Netherlands*

[3] *Universiteit van Amsterdam, Department of Chemical Engineering, Nieuwe Achtergracht 166, 1018 WV Amsterdam, The Netherlands*

Abstract

In this paper we present a shooting method in combination with a hybrid Newton-Picard method to compute efficiently the periodic states of cyclically operated chemical processes. The merits of the method are investigated by considering the computation of the periodic states of a rapid pressure swing adsorption systems and of a cooled reverse flow reactor. We show that these periodically forced chemical processes exhibit low dimensional dynamics. The Newton-Picard method is designed to make efficient use of this low dimensional dynamics of the chemical processes. In addition the Newton-Picard method is able to determine the stability of the computed periodic states. As an illustration of the efficiency of the method, we compute a branch of periodic states for the reverse flow reactor.

KEYWORDS: Periodic solutions, periodic forcing, cyclic chemical processes, Newton-Picard method

1. Introduction

Many processes in the chemical industry are operated under periodically varying, dynamic conditions. Examples of such processes are the temperature swing and pressure swing separation processes, the simulated moving bed reactor-separator, the reverse flow reactor, and the more recently developed pressure swing reactor.

*Corresponding author. e-mail: verduyn@math.leidenuniv.nl

The common feature of these processes is that the model equations are usually reaction-convection-diffusion equations with time periodic coefficients and time periodic boundary conditions.

The solutions to these equations that are theoretically *and* practically the most interesting are the solutions that correspond to the limiting states of the process. The motivation to study and compute these solutions is that they determine the states a process will be in for most of the time, after an initial transient start-up phase. The efficient determination of the limiting states is therefore of great importance for the understanding, design and optimization of chemical processes. Whereas for the traditional steady state operated reactors, the limiting state is often time invariant, the limiting state of a cyclic process is inherently dynamic in nature. The typical limiting state of a cyclic process is a so-called *cycle invariant* or *periodic* state. Because of the time dependent characteristics, the numerical determination of periodic states is not a simple task.

A natural and obvious way to calculate a periodic state of a cyclic process is to simulate its dynamic behaviour. The simulation will approach, as does the physical system, a periodic state. The disadvantage of this approach is that the initial transient phase may be very long, in particular, in the presence of large capacity terms and slow kinetic terms. All example reactor types given above are based on packed beds, where a column is filled with a solid sorbent and/or catalyst. Typically the solids inventory is very high and so is the buffer capacity in terms of the adsorption capacity or heat capacity. For such systems the dynamic simulation of the process may need tens of thousands of cycles in order to converge to a periodic state. In optimization problems, where these calculations need to be carried out numerous times, the fact that dynamic simulations are grossly inefficient becomes a serious problem. Actually, this long transient phase enforces the use of over-simplified models to be able to do any computations at all within a reasonable CPU time.

In the last decade a number of efficient numerical methods have been suggested and discussed in the chemical engineering literature. One of the first papers on convergence acceleration methods for cyclic processes was published by Smith IV and Westerberg (1992). In this paper, the authors use Broyden's method to accelerate the convergence for a linear pressure swing adsorption (PSA) system. This method yields acceleration factors ranging from roughly 3 to 50.

Croft and Levan (1994) propose Newton's method to compute periodic states. The derivative of the period map of the process needed for the Newton iterations is calculated using the variational equations. This method only accelerates the convergence for systems that converge slowly to a periodic state. The method also allows for the calculation of periodic states satisfying some further design constraints.

Yet another method was proposed by Salinger and Eigenberger (1996). In their work the authors present the so-called double discretization method or relaxation method. In this approach, the axial space axis and time axis are discretized simultaneously, using a finite elements method and the periodic boundary conditions are imposed directly. This leads to a large system of algebraic equations that can be solved using standard methods. The relaxation method was used to compute periodic states of a reverse flow reactor (RFR) and also in a bifurcation analysis of this reactor. The main drawback of the relaxation method is the large computer memory requirements. This is related to the fact that the size of the Jacobian, that has to be calculated when a Newton type algorithm is used to solve the large system of algebraic equations, grows quadratically with the number of equations.

None of the methods in the above cited references uses any characteristic of the underlying chemical processes: the methods are designed to work for *general* periodically forced systems of partial differential equations. In the present paper we give numerical evidence that the chemical processes under consideration exhibit low dimensional dynamics. We will discuss a single shooting method in combination with a hybrid Newton-Picard method that uses the low dimensional dynamics of the chemical processes for the efficient determination of their periodic states. This method is developed by Lust et al. (1998) and is used to compute periodic solutions of large systems of autonomous ordinary differential equations, autonomous partial differential equations and delay differential equations. We will apply a variant of this method to compute periodic states of a rapid pressure swing adsorption system and a cooled reverse flow reactor. Other applications, for example, to pressure swing adsorbers and reverse flow reactors and a comparison of the Newton-Picard method to Broyden's method, dynamic simulation and Newton's method can be found in (Van Noorden et al., 1999) and (Van Noorden et al., 2001). In the present paper, the main focus is to show that cyclically operated chemical processes exhibit low dimensional dynamics which makes them well suited for the Newton-Picard method. As an illustration of the efficiency of the method we compute a branch of periodic solutions of the reverse flow reactor.

The organization of this paper is as follows. In Section 2 we present and discuss models for the rapid pressure swing adsorber and the reverse flow reactor. In Section 3 we present the Newton-Picard method and show that the cyclically operated chemical processes introduced in Section 2 exhibit low dimensional dynamics. In Section 4 we compute the periodic states of the rapid pressure swing adsorption system and the reverse flow reactor using the Newton-Picard method.

2. Two Example Systems

In this section we discuss the models of a reverse flow reactor and of a rapid pressure swing adsorption system. The parameters in this section are all dimensionless. The relation between the dimensionless and the physical parameters are given in an appendix.

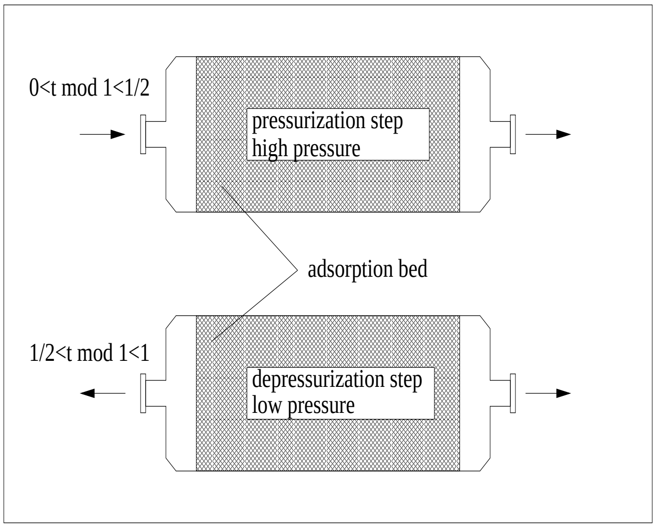

Figure 1: A rapid pressure swing adsorber.

2.1. The Rapid Pressure Swing Adsorber

Pressure swing adsorption processes are systems that separate mixtures of gases by periodically varying the pressure over an adsorption bed (See Fig. 1). Among the pressure swing adsorption processes, the Rapid Pressure Swing Adsorption process (RPSA) offers one of the simplest configurations. The RPSA cycle comprises two basic steps: pressurization by feed gas and countercurrent depressurisation with internal purging. Both steps have a short time duration, in the order of several seconds. The adsorption bed consists of small adsorbent particles with average size (between 200-700 μm). The effectiveness of self purging within the RPSA bed results from a combination of a fast cycle time together with a small particle size leading to steep and periodically varying pressure gradients within the bed. The pressure at the product end is approximately constant over time and this makes the process useful for continuous product release.

The specific process of interest to this case study is air purification using an adsorption bed of zeolite A5 which preferentially adsorbs nitrogen and leaves oxygen in the product stream. The model is taken from (Nilchan and Pantelides, 1998).

The model gas consists of two components, oxygen and nitrogen. The variables in the model are the gas phase concentrations of these two components, denoted by $c^{(i)}(t,x) : [0,\infty) \times [0,1] \to [0,\infty)$ ($i = 1$: oxygen, $i = 2$: nitrogen), the adsorbed amount of the two components, denoted by $q^{(i)}(t,x) : [0,\infty) \times [0,1] \to [0,\infty)$ and the gas phase velocity $v(t,x) : [0,\infty) \times [0,1] \to \mathbb{R}$. The dimensionless parameters that appear in the equations are denoted by C_1, C_2, $C_3^{(i)}$, C_4, C_5, $k^{(i)}$, $D^{(i)}$, $y_f^{(i)}$, p_w and t_f. Their values are listed in Table 1. The model equations consist of the gas phase balance equations

$$c_t^{(i)} = C_1 c_{xx}^{(i)} - C_2 (v c^{(i)})_x - C_3^{(i)} q_t^{(i)}, \tag{1}$$

for $i = 1, 2$, the adsorption rate equations

$$q_t^{(i)} = \frac{k^{(i)}}{c^{(1)} + c^{(2)} + D^{(i)}} (c^{(i)} - q^{(i)}). \tag{2}$$

and the gas phase velocity equation

$$v(t, x) = -C_4 (c_x^{(1)}(t, x) + c_x^{(2)}(t, x)). \tag{3}$$

Note that the equations are autonomous, but the boundary conditions are periodic in time. In fact, at the feed end (at $x = 0$) of the adsorber there are two sets of alternating boundary conditions. During the first step, the so-called *pressurization step*, the boundary conditions are

$$\begin{cases} c_x^{(i)}(t,0) = C_1^{-1} C_2 v(t,0)(c^{(i)}(t,0) - y_f^{(i)}) \\ c^{(1)}(t,0) + c^{(2)}(t,0) = 1 \end{cases} \quad \text{for } 0 \le t \,(\text{mod } 1) < t_f. \tag{4}$$

During the second step, the so-called *depressurization step*, the boundary conditions are

$$\begin{cases} c_x^{(i)}(t,0) = 0 \\ c^{(1)}(t,0) + c^{(2)}(t,0) = p_w \end{cases} \quad \text{for } t_f \le t \,(\text{mod } 1) \le 1. \tag{5}$$

In this formulation we have rescaled to cycle time to become one time unit. The boundary conditions at the product end (at $x = 1$) of the adsorber are given by

$$\begin{cases} c_x^{(i)}(t,1) = 0 \\ v(t,1) = C_5 (c^{(1)}(t,1) + c^{(2)}(t,1))^{-1} \end{cases} \tag{6}$$

The equations (1)-(3) together with the boundary conditions (4)-(6) complete the description of the RPSA model. A solution of (1)-(3) together with the boundary conditions (4)-(6) that satisfies

$$\begin{cases} c^{(i)}(0,\cdot) = c^{(i)}(1,\cdot) \\ q^{(i)}(0,\cdot) = q^{(i)}(1,\cdot) \end{cases} \quad i = 1, 2,$$

is called a periodic solution of the RPSA model.

2.2. The Cooled Reverse Flow Reactor

A Reverse Flow Reactor (RFR) is a packed bed reactor in which the flow direction is periodically reversed to trap a hot zone within the reactor (see Fig. 1). In this way exothermic reactions can be operated without preheating the

Table 1: The dimensionless parameter values for the RPSA process

C_1	0.0042	C_2	1.4134
$C_3^{(1)}$	3.8988	$C_3^{(2)}$	8.3975
C_4	1.8470	C_5	0.0072
$k^{(1)}$	438.2138	$k^{(2)}$	203.4564
$D^{(1)}$	0.5351	$D^{(2)}$	0.5007
$y_f^{(1)}$	0.21	$y_f^{(2)}$	0.79
p_w	0.4717	t_f	0.5

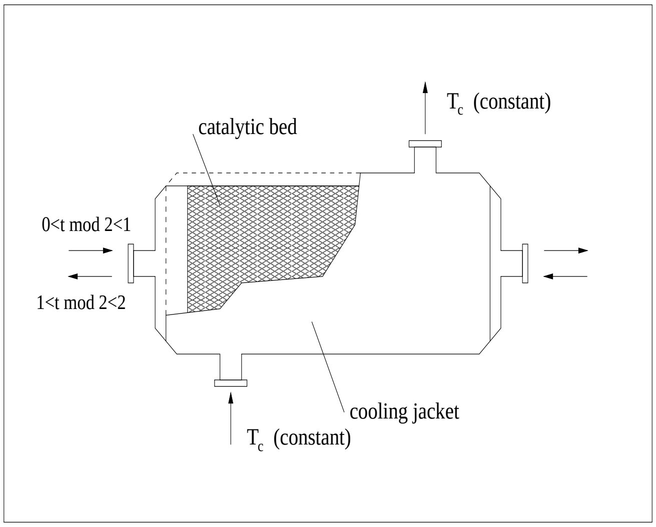

Figure 2: Cooled reverse flow reactor.

feed stream. We consider a cooled RFR in which a single irreversible, exothermic, first order reaction occurs. We describe the RFR by a one-dimensional, pseudo-homogeneous model that accounts for axial heat and mass dispersion and external mass transfer resistance between the fluid and the catalyst. The basic model assumption is to assume that all the physical properties are independent of the temperature and the concentration. The model is taken from (Khinast et al., 1998).

The variables in the model are the dimensionless temperature $\theta(t,x) : [0,\infty) \times [0,1] \to [0,\infty)$ and the conversion $\chi(t,x) : [0,\infty) \times [0,1] \to [0,1]$. The dimensionless parameters that appear in the model equations are denoted by K_j for $j = 1,..,7$ and by $g(\theta(t,x))$. The model specific values are given in Table 2. For flow from left to right the dimensionless energy and species balances reads

$$\theta_t = K_1\theta_{xx} - K_2\theta_x + K_3 g(\theta)(1-\chi) + K_4(1-\theta), \qquad (7)$$

$$\chi_t \quad = \quad K_5\chi_{xx} - K_6\chi_x + K_7 g(\theta)(1-\chi). \tag{8}$$

with boundary conditions

$$\begin{array}{cc} K_1\theta_x(t,0) = K_2(\theta(t,0)-1), & K_5\chi_x(t,0) = K_6\chi(t,0), \\ \theta_x(t,1) = 0, & \chi_x(t,1) = 0. \end{array} \tag{9}$$

At each integer value of t the flow direction reverses and the evolution equations and the boundary conditions change accordingly. A *cycle* consists of two flow reversals. This means that one cycle has a duration of two time units. The equations (7)-(8) with the boundary conditions (9) describe the model.

A periodic state of (7)-(8) with the boundary conditions (9) is a solution that satisfies

$$\begin{aligned} \theta(0,x) &= \theta(1,1-x), \\ \chi(0,x) &= \chi(1,1-x). \end{aligned}$$

Thus a periodic solution consist of two symmetric parts of one time unit. The values of the dimensionless parameters are given in Table 2.

Table 2: The dimensionless parameter values for the reverse flow reactor

K_1	$6.9393{\cdot}10^{-4}$	K_2	0.1749
K_3	$1.5577{\cdot}10^{-6}$	K_4	varied (0-8000)
K_5	$2.4038{\cdot}10^{-3}$	K_6	174.06
K_7	0.01	$g(\theta)$	$\dfrac{1.6656\cdot 10^{-5}e^{25.785(\theta-1)/\theta}}{1.6656\cdot 10^{-5}+e^{-25.785/\theta}}$

3. A Newton-Picard Shooting Method for Periodically Forced Systems

The models for the chemical systems discussed in Section 2, are given in term of partial differential equations. In order to investigate the behaviour of these systems numerically, we first have to discretize the equations. For the shooting method, first the spatial variable of the equations is discretized. This results in a large system of N (where N depends on the space discretization) time periodic ordinary differential equations. This system can abstractly be written as

$$x'(t) = f(t, x(t)) \ , \ \text{ where } \ f(t+T,\cdot) = f(t,\cdot) \ , \tag{10}$$

where $x(t) = (x_1(t), x_2(t), \ldots, x_N(t))$ is a N-dimensional vector. The right hand side, denoted by f, of the ordinary differential equation (10) has the following additional structure. If a finite element or finite difference discretization is used to discretize the spatial variable, then the components of x can usually be ordered in such a way that the Jacobian of f has a band structure. Secondly, as we have seen in the model equations in Section 2, the time variable t can always be rescaled in order to make the period T of the periodic forcing in f equal to one.

The map $F : \mathbb{R}^N \to \mathbb{R}^N$ that assigns to the initial data at time zero, $x(0) = x_0$, the value of the solution after one cycle, i.e., the state $x(T)$, is called the Poincaré or period map of (10)

$$F(x_0) = x(T, x_0), \tag{11}$$

where $x(t, x_0)$ denotes the solution of (10) with initial condition $x(0) = x_0$. So, evaluating the map F is equivalent to integrating the system (10) over a period of time with length T starting with a given initial condition x_0.

A periodic state of the chemical system is a T-periodic solution $x(t)$, i.e., a solution with $x(0) = x(T)$, of (10), and therefore the initial condition of a periodic solution is a fixed point of the equation $x = F(x)$. The stability of a periodic solution of (10), or equivalently, a fixed point x^* of F, is determined by the eigenvalues of the Jacobian $J(x^*)$ of F at the fixed point x^*.

When a periodic state $x(t, x^*)$ is stable, i.e. all the eigenvalues of the Jacobian $J(x^*)$ of F at the fixed point x^* are inside the open unit disc $C := \{z \in \mathbb{C} : |z| < 1\}$, then the periodic state can be obtained by integrating eq. (10) on a long time interval, starting with an initial condition that is sufficiently close to the periodic solution. This approach is equivalent with a Picard iteration of the map F which is, in many cases, not feasible. As noted in the introduction, the convergence to a periodic state of a dynamic simulation can be very slow. Furthermore, only *stable* periodic states can be obtained by this approach.

A Newton-like method, applied directly to the fixed point equation, would allow to compute both stable and unstable periodic states. However such an approach involves the computation or approximation of the Jacobian $J(x)$ of F at various points x, either by numerical differentiation or by solving the variational form of (10). Both approaches are very expensive when N is large (Lust et al., 1998) (Croft and Levan, 1994). Note that, in contrast to the map f in the right hand side of (10), the Jacobian of the map F does generally not have a band structure.

Since the value $F(x_0)$ is obtained by integrating a large system of differential equations over a period of time with initial condition x_0, the evaluation of F is a computationally expensive task. This means that for any method used to find a fixed point of F, most of the computation time will be spent in the evaluation of F. Thus the method that needs the least number of evaluations of F will be the most efficient method. The main idea behind the Newton-Picard method, discussed in the next section, is to minimize the number of function evaluations.

3.1. The Newton-Picard Method

The philosophy underlying a hybrid Newton-Picard method (Lust et al., 1998), (Shroff and Keller, 1993) is that many (infinite dimensional) physically interesting systems exhibit low dimensional dynamics. By this we mean that the number of large eigenvalues of the Jacobian $J(x)$ of F at various points x is small, and essentially independent of the discretization. The numerical computation of the eigenvalues of the Jacobian $J(x)$ for the two model systems discussed in Section 2, shows that this assumption of low dimensional dynamics also holds for these two infinite dimensional systems. For typical plots of the eigenvalues of $J(x)$ see Figures 4 and 6 in Section 4. The fact that there are only a small number of large eigenvalues, means that we can avoid the explicit calculation of the Jacobian J of F, and only compute the action of J on a p dimensional subspace of $\mathbb{R}^N$, where p is much smaller than N.

The Newton-Picard method is a quasi-Newton method. This means that the method produces approximations to a fixed point of F, using the iteration scheme

$$\begin{cases} x_{i+1} = x_i + \Delta x_i \text{ with} \\ \Delta x_i \approx -(J(x_i) - I)^{-1}(F(x_i) - x_i), \end{cases} \tag{12}$$

where $J(x_i)$ denotes the Jacobian of F at x_i.

Fix i, set $x = x_i$ and assume that the eigenvalues μ_1, μ_2, ..., μ_N of $J(x)$ are known, ordered by decreasing modulus

$$|\mu_1| \geq |\mu_2| \geq ... \geq |\mu_p| > \rho > |\mu_{p+1}| \geq ... \geq |\mu_N|,$$

where ρ is a free parameter of the method. Define U to be the subspace of the discretized state space $\mathbb{R}^N$ spanned by the eigenvectors and generalized eigenvectors of $J(x)$ corresponding to the eigenvalues μ_k, $k = 1, ..., p$. Let $V_p \in \mathbb{R}^{N\times p}$ denote an orthogonal basis of U, i.e., the columns of V_p are orthogonal and span the subspace U. Finally, let $V_q \in \mathbb{R}^{N\times(N-p)}$ be an orthogonal basis of $U^\perp$, the orthogonal complement of U in $\mathbb{R}^N$.

The idea is to decompose the correction Δx into a component in U and a component in $U^\perp$. For this decomposition we construct the orthogonal projectors $P := V_p V_p^T$ onto U, where V_p^T denotes the transpose of the matrix V_p and $Q := V_q V_q^T = I - P$ onto $U^\perp$. Consequently, the correction can be written as

$$\Delta x = P\Delta x + Q\Delta x = V_p V_p^T \Delta x + V_q V_q^T \Delta x = V_p \Delta\bar{p} + V_q \Delta\bar{q}, \tag{13}$$

where the notation $\Delta\bar{p} := V_p^T \Delta x$ and $\Delta\bar{q} := V_q^T \Delta x$ is used.

We would like Δx to be an approximate solution of

$$(J(x) - I)\Delta x = -(F(x) - x). \tag{14}$$

So we substitute (13) in (14) and multiply the left and right hand side of (14) by $(V_p \;\; V_q)^T$. This leads to the matrix equation

$$\begin{pmatrix} V_p^T(J(x) - I)V_p & V_p^T J(x) V_q \\ 0 & V_q^T(J(x) - I)V_q \end{pmatrix} \begin{pmatrix} \Delta\bar{p} \\ \Delta\bar{q} \end{pmatrix} = -\begin{pmatrix} V_p^T(F(x) - x) \\ V_q^T(F(x) - x) \end{pmatrix}.$$

Note that the last row of this equation does not contain an expression in $\Delta\bar{p}$. Therefore this row (which contains $N-p$ equations) can be solved for $V_q\Delta\bar{q}$ with the Picard iteration scheme

$$V_q\Delta\bar{q}_{j+1} = V_qV_q^TJ(x)V_q\Delta\bar{q}_j + V_qV_q^T(F(x)-x). \tag{15}$$

If the approximation of the solution of (15) is again denoted by $V_q\Delta\bar{q}$, then the equation for $\Delta\bar{p}$ becomes

$$V_p^TJ(x)V_q\Delta\bar{q} + V_p^T(J(x)-I)V_p\Delta\bar{p} = -V_p^T(F(x)-x).$$

Solving this equation only requires the evaluation of F, i.e., one cycle simulation, p times.

Together $V_q\Delta\bar{q}$ and $V_p\Delta\bar{p}$ make up the update in the scheme (12), which , with the decomposition made in (13), can be written as

$$x_{i+1} = x_i + V_p\Delta\bar{p} + V_q\Delta\bar{q}.$$

Because of the way the two subspaces U and $U^\perp$ are constructed, the scheme (15) will converge much faster than the direct substitution method applied to the original system of equations. We refer to (Lust et al., 1998) for more details about the convergence analysis of the method.

The dimension p of U is and an initial approximation to a basis V_p of the subspace U is obtained by computing before the first Newton-Picard iteration the Jacobian with finite differences and calculating its eigenvalues and eigenvectors. The eigenvectors and generalized eigenvectors corresponding to the p largest eigenvalues span the subspace U. An orthogonal basis can be obtained using a Gram-Schmidt orthogonalization procedure. Notice that since the Jacobian is available for this first iteration, we can take the first iteration to be a Newton iteration. In the subsequent iterations of the Newton-Picard algorithm, the basis of the subspace U is updated with one subspace iteration with projection (the details of this subspace iteration procedure with projection can be found in (Lust et al., 1998); see also (Saad, 1992)). It is important to note that in this subspace iteration, approximations to the p largest eigenvalues of the Jacobian are obtained. These eigenvalues are essential in the determination of the stability of a periodic state.

In contrast to the approach of Lust et al. (1998), where the subspace iteration is performed on $p + p_e$ (with $p_e = 2$, 3 or 4) vectors in order to accelerate the convergence of the subspace iteration procedure and to aid the detection of eigenvalues leaving or entering the region $C_\rho := \{z \in \mathbb{C} : |z| < \rho\}$, we only perform the subspace iteration on p vectors, and fix the dimension of the subspace U before the first iteration of the Newton-Picard algorithm. This approach creates of course the problem that at a certain point in the iteration procedure eigenvalues may exist that:

1) have moved out of C_ρ, but of which the corresponding eigenvector is not in the subspace U or

2) have moved into C_ρ, but of which the corresponding eigenvector is still in U.

Case 2) is not a real problem: it will only cause the Picard iteration in eq. (15) to converge even faster). In Case 1) the Picard iteration in eq. (15) slows down and in the worst case, when an eigenvalue as moved unnoticed out of the unit disk C, it will not converge at all. These problems can be overcome by a procedure that monitors the convergence rate of the Picard iterations in eq. (15) and adjusting the dimension of U accordingly. This approach is used in (Shroff and Keller, 1993) and (Jarausch and Mackens, 1984). In our computations for the systems described in Section 2 we did not need to use such a monitoring procedure: we fixed the dimension of the subspace U before the first Newton-Picard iteration and our test systems were well behaved in the sense that with this strategy we did not encounter problems of the kind described in Case 1) above. But for more wildly behaving systems with eigenvalues that change rapidly, a monitoring procedure as used in (Shroff and Keller, 1993) and (Jarausch and Mackens, 1984) or the approach in (Lust et al., 1998) is necessary.

Another difference between our approach and that of Lust et al. (1998) is that we do not use locking and deflation in the subspace iteration and that the matrix-vector products $J(x_i)v_j$, $J(x_i)V_{p_i}$ and $J(x_i)(V_q\Delta\bar{q})$ in the steps 6), 7) and 8) in the algorithm below, are calculated using a finite difference approximation given by

$$J(x)v \approx \frac{1}{\epsilon}(F(x+\epsilon v) - F(x)).$$

The Newton-Picard algorithm as implemented, performs a fixed number of iterations of the Picard scheme (15). This number is denoted by l in the following description of the steps of the algorithm. The number δ_0 in step 5) is the bound for convergence to a periodic state. In parenthesis, we denote the number of F-evaluations that is needed.

Newton-Picard Algorithm

1) *Choose an initial value* x_0.
2) *Compute the Jacobian* $J(x_0)$ *of* F *at* x_0 *(finite differences:* $N+1$ F*-evaluations).*
3) *Compute the eigenvalues and eigenvectors of* $J(x_0)$. *This determines* p, *the dimension of the slow subspace* U *and an orthonormal basis* V_p *of* U.
4) $x_1 = x_0 - (J(x_0) - I)^{-1}(F(x_0) - x_0)$.
5) *If* $|F(x_i) - x_i| < \delta_0$ *then stop (1* F*-evaluation).*
6) $v_0 = (I - V_{p_i}V_{p_i}^T)(F(x_i) - x_i)$. *Iterate* $v_{j+1} = (I - V_{p_i}V_{p_i}^T)(J(x_i)v_j + (F(x_i) - x_i)$ l *times. Set* $V_q\Delta\bar{q} := v_l$. *(Computation of* $J(x_i)v_j$: l F *evaluations).*
7) *Compute* $S := J(x_i)V_{p_i}$ *(*p F*-evaluations).*

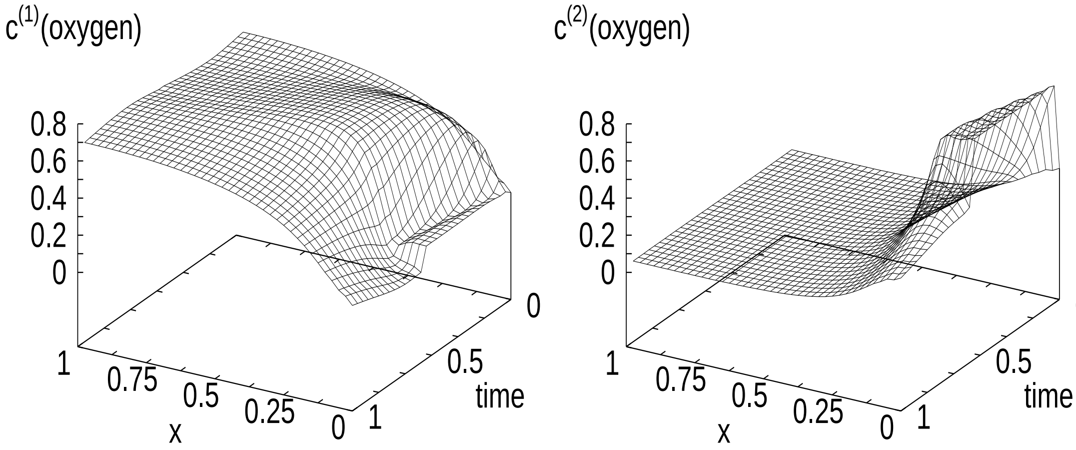

Figure 3: The computed periodic state for the rapid pressure swing adsorber: the dimensionless gas phase concentration of oxygen (left) and nitrogen (right) versus the axial distance x and time.

8) Solve $(V_{p_i}^T S - I)(\Delta\bar{p}) + V_{p_i}^T J(x_i)(V_q \Delta\bar{q}) = -V_{p_i}^T (F(x_i) - x_i)$ *for* $\Delta\bar{p}$. *(Computation of* $J(x_i)(V_q\Delta\bar{q})$*: 1* F*-evaluation).*

9) Set $x_{i+1} := x_i + V_{p_i}\Delta\bar{p} + V_q\Delta\bar{q}$.

10) Compute the ordered real Schur-factorization $Y^T R Y$ *of* $V_{p_i}^T S$*. Compute* $V = SY$*. Orthonormalize* V *and put the result in* $V_{p_{i+1}}$*. Go to step 5).*

The above algorithm amounts to $p + 2 + l$ cycles per iteration. In our implementation we take $l = 2$. Thus, for each iteration of the Newton-Picard method, we need $p + 4$ cycle simulations. We will end this section with a remark about the extreme values, 0 and 1, of the parameter ρ. The parameter ρ determines the dimension of the subspace U. If we set ρ equal to one for determining a stable fixed point of F, then U is empty and the Newton-Picard method reduce to Picard iteration of the map F. On the other hand, if we set ρ equal to 0, then U equals the whole of $\mathbb{R}^N$, and the Newton-Picard method reduces to Newton's method.

4. Computation of the periodic states

In this section the Newton-Picard method is used to compute periodic states of the rapid pressure swing adsorption process and of the reverse flow reactor. All the computations presented in this section were done on a Linux desktop computer.

4.1. The Rapid Pressure Swing Adsorber

For the rapid pressure swing adsorber we chose to discretize the spatial variable on a grid of 100 nodes using a finite volume approach with second order centered

Table 3: The number of cycle simulations for the different values of ρ for the rapid pressure swing adsorber.

$\rho = 1$ (Picard)	$\rho = 0.75$	$\rho = 0.5$	$\rho = 0.25$	$\rho = 0$ (Newton)
3278	666	560	550	2009

Table 4: The dimension of U for each values of ρ for the rapid pressure swing adsorber.

$\rho = 0.75$	$\rho = 0.5$	$\rho = 0.25$
6	10	14

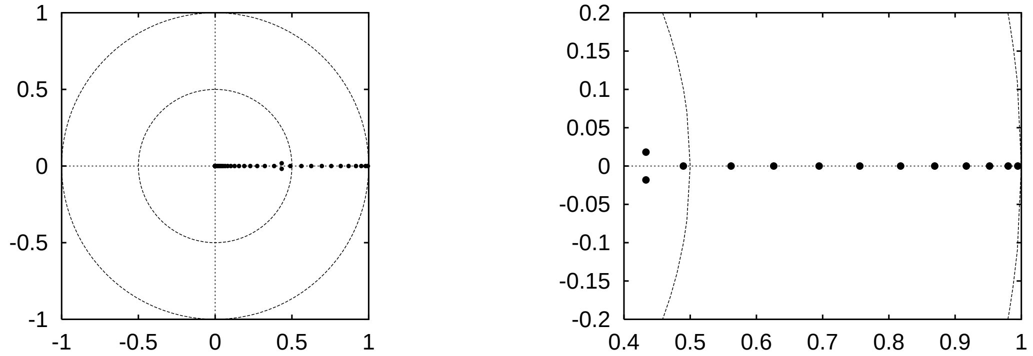

Figure 4: The eigenvalues of the Jacobian $J(x^*)$ for the rapid pressure swing adsorber at the periodic state x^* of the (discretized) infinite dimensional period map F plotted in the complex plane. In the right figure we zoom in on the eigenvalues close to 1.

finite differences. After the spatial discretization of the two mass balances and the two adsorption rate equations, a system of 400 ordinary differential equations is obtained and hence $N = 400$. The system of ODE's is integrated in time using the NAG fortran library routine D02EJF. For the δ_0 in the convergence criterion in the Newton-Picard method we take $\delta_0 = 10^{-9}$.

In order to show that the rapid pressure swing adsorber exhibits low dimensional dynamics, in Figure 4 a typical plot of the eigenvalues of the Jacobian is depicted. We see that there are only 10 eigenvalues out of the computed 400, that are outside the disc with radius 0.5.

We would like to determine a periodic state for the parameter values given in Table 1. The initial conditions for the computations are given by

$$c^{(i)}(0, x) = q^{(i)}(0, x) = y_f^{(i)} p_w.$$

The optimal choice of the parameter ρ in the Newton-Picard method depends on the problem under consideration. There are no good rules for making the

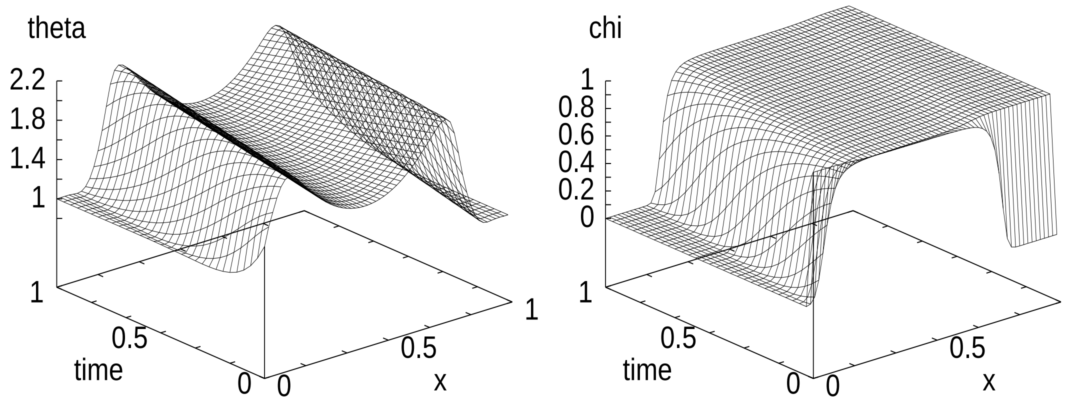

Figure 5: The computed periodic state for the reverse flow reactor with the dimensionless cooling capacity $K_4 = 1750$: the dimensionless temperature θ (left) and the conversion χ (right) versus the axial distance x and time.

choice, except a rule of thumb gathered from experience: Lust et al. (1998) report that values of ρ around 0.5 result in good performance of the method.

We applied the Newton-Picard method for several values of ρ. The number of F-evaluations needed for the computation of the periodic state for these values of ρ are listed in Table 3. In Table 4 for each value of ρ the corresponding dimension of the subspace U is given. We see that for ρ equal to 0.5 and 0.25 the method is most efficient, which is in agreement with the experiences of Lust et al. (1998).

The computed periodic state is depicted in Figure 3.

4.2. The Cooled Reverse Flow Reactor

For the reverse flow reactor we chose to discretize the spatial variable on a grid of 120 nodes using a finite volume approach with upwinding of the first space derivatives in the mass balance . The discretization of the model equations results for the RFR in a system of 240 ordinary differential equations. Hence $N = 240$. The system of ODE's is integrated in time using the NAG fortran library routine D02EJF. The δ_0 in the Newton-Picard method is taken to be 10^{-7}.

In order to show that the reverse flow reactor also exhibits low dimensional dynamics, in Figure 6 a typical plot of the eigenvalues of the Jacobian is depicted. We see that there are only 9 eigenvalues out of the computed 240, that are outside the disc with radius 0.5.

We applied the Newton-Picard method to compute a periodic state of the reverse flow reactor for two different values of the parameter K_4, i.e. $K_4 = 0$ and $K_4 = 1750$. The parameter K_4 is a dimensionless measure for the cooling capacity, with $K_4 = 0$ corresponding to no cooling. For both computations the

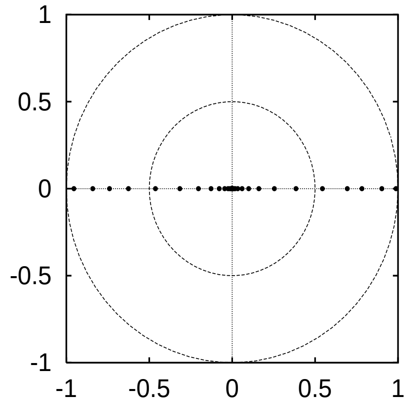

Figure 6: The eigenvalues of the Jacobian $J(x^*)$ for the reverse flow reactor with $K_4 = 0$ at the periodic state x^* of the (discretized) infinite dimensional period map F plotted in the complex plane.

initial conditions

$$\theta(0, x) = 2.02 \text{ and } \chi(0, x) = 0.7,$$

were used. In Table 5 the number of function evaluations for the different values of ρ are listed and in Table 6 the corresponding dimension of the subspace U is given. We see that for both values of K_4 the method is most efficient with $\rho = 0.5$. For $K_4 = 1750$, however, the differences between the various computations is small, and even the Picard iteration ($\rho = 1$) performs well.

Table 5: The number of cycle simulations for the different values of ρ for the reverse flow reactor.

	$\rho = 1$ (Picard)	$\rho = 0.75$	$\rho = 0.5$	$\rho = 0.25$	$\rho = 0$ (Newton)
$K_4 = 0$	991	396	337	365	1211
$K_4 = 1750$	346	376	324	331	729

As the Newton-Picard method is designed to perform especially well in a continuation context we did not only compute single periodic states for the reverse flow reactor, but also a branch of periodic states for a range of values of the parameter K_4. The parameter K_4 was varied in 81 steps from 0 to 8000. Only for the first periodic state (for $K_4 = 0$) the Jacobian of F and the basis V_p of the subspace U was computed. After that the basis V_p at the end of the previous value of K_4 is used as an approximation of the basis at the new value of K_4. As initial condition the state computed at the previous vale of K_4 was used. For each value of K_4 also the three eigenvalues of J with the largest absolute value were computed with four digits of accuracy. For this purpose after the Newton-Picard iterations in most cases only one subspace iteration was sufficient.

In Figure 7 the branch of periodic states is depicted. In the left figure the maximum temperature in the bed at flow reversal is plotted versus K_4. In the right figure for each value of K_4 the eigenvalues with largest absolute value are plotted.

Table 6: The dimension of U for each values of ρ for the reverse flow reactor.

	$\rho = 0.75$	$\rho = 0.5$	$\rho = 0.25$
$K_4 = 0$	6	9	13
$K_4 = 1750$	6	9	13

We computed the branch of periodic states with three different choices for the dimension of U. The number of F-evaluations used in these three computations is given in Table 7. The run with dimension 9 for U is the most efficient (this value corresponds to $\rho = 0.5$ for the first iteration). For this run the average number of F-evaluations needed for each value of K_4 is less than 80. This is about one third of the computational effort of one Newton iteration ($N = 240$).

Table 7: The number of function evaluations for the different runs of the parameter continuation for the reverse flow reactor.

dim. of U	number of eval.
6	9335
9	6408
12	6853

5. Conclusions

In this paper we have discussed two cyclically operated chemical processes, a rapid pressure swing adsorber and a reverse flow reactor. We have shown that these systems exhibit low dimensional dynamics which makes them well suited for the Newton-Picard method for the efficient computation of their periodic states.

The Newton-Picard method that we have described in this paper applies to periodically forced systems of reaction/convection/diffusion equations with time periodic coefficients and time periodic boundary conditions and is a variant of the method described in (Lust et al., 1998). A difference to the approach in (Lust

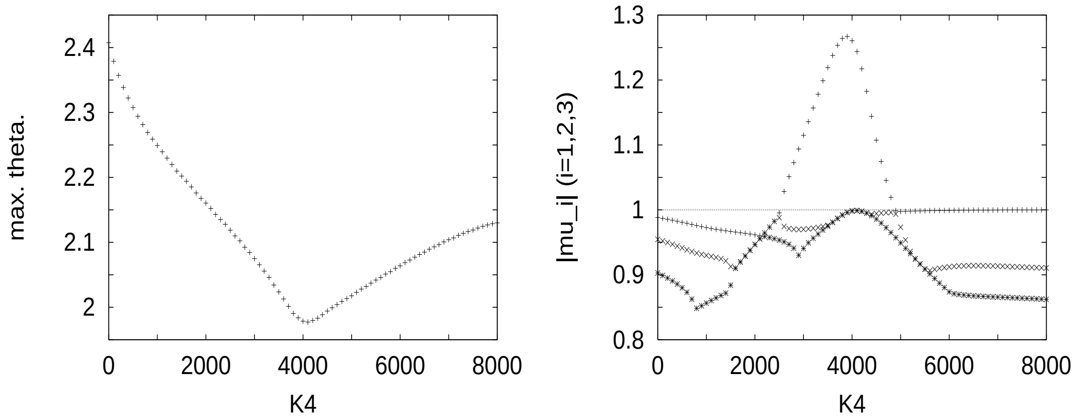

Figure 7: The computed branch of periodic solutions for the reverse flow reactor: the maximum temperature in the bed at flow reversal (left) and the moduli of the three eigenvalues $|\mu_i|$ $(i = 1, 2, 3)$ of the Jacobian J at the periodic state with the largest absolute values (right) versus K_4.

et al., 1998) is that we keep the dimension of the subspace U, the part of the state space $\mathbb{R}^N$ on which the action of the Jacobian is computed, fixed. Another difference is that we perform the subspace iterations, which update the basis of the subspace U, only on p (the dimension of U) vectors.

We have applied the method to the two presented cyclic chemical systems. For these systems we have shown that the Newton-Picard method is much more efficient than either a Picard method or a Newton's method. The Newton-Picard method is also able to compute accurately the largest eigenvalue of the Jacobian of the period map at the periodic solutions, and is thus able to determine the stability of these solutions.

In ongoing work we plan to use the Newton-Picard algorithm in combination with a pseudo-arclength parameterization method and compare the performance of the method with a Broyden scheme that is adapted for the computation of the dominant eigenvalues of the Jacobian of the period map.

A. Parameters for the Rapid Pressure Swing Adsorber

The dimensionless parameters are given by

$$
\begin{aligned}
C_1 &= D_{ax}T/L^2, \\
C_2 &= 1/(\varepsilon_b + \varepsilon_p(1-\varepsilon_b)), \\
C_3^{(i)} &= \rho_b m_i R T_0/(\varepsilon_b + \varepsilon_p(1-\varepsilon_b)), \\
C_4 &= T d_p^2 \varepsilon_b^3 P_f/(180\mu(1-\varepsilon_b)^2 L^2), \\
C_5 &= Q P_{atm} T/(A P_f L), \\
D^{(i)} &= D_m/D_k^{(i)}, \\
k^{(i)} &= 60 T \varepsilon_p^2 (1-\varepsilon_b) D_m/(d_p^2 \rho_b m_i R T_0 \tau_p),
\end{aligned}
$$

$$p_w = P_{atm}/P_f$$

The values of the physical parameters are given in Table 8.

Table 8: The physical parameter values for the RPSA process. Super- or subscript 1 denotes oxygen, 2 denotes nitrogen.

D_{ax}	10^{-3} m^2/s	axial dispersion coefficient
D_m	$9.376 \cdot 10^{-6}$ m^2/s	molecular diffusion coefficient
m_1	$3.08 \cdot 10^{-6}$ m^2 mol/(N kg)	adsorption isotherm coefficient
m_2	$1.43 \cdot 10^{-6}$ m^2 mol/(N kg)	adosorption isotherm coefficient
P_{atm}	$1.013 \cdot 10^5$ N/m^2	atmospheric pressure
P_f	$2.148 \cdot 10^5$ N/m^2	feed pressure
d_{pore}	$0.12 \cdot 10^{-6}$ m	pore diameter
$y_f^{(1)}$	0.21 (-)	feed oxygen mole fraction
$y_f^{(2)}$	0.79 (-)	feed nitrogen mole fraction
ε_p	0.55 (-)	adsorbent void fraction
ε_b	0.35 (-)	bed void fraction
Q	10^{-5} m^3/s	product delivery rate
ρ_b	800 kg/m^3	bed bulk density
μ	$1.8 \cdot 10^{-5}$ N s/m^2	gas viscosity
τ_p	3 (-)	particle tortuosity factor
L	1 m	bed length
d_p	$3.025 \cdot 10^{-4}$ m	particle size
T	3 s	cycle time
$D_k^{(1)}$	$1.752 \cdot 10^{-5}$ m^2/s	knudsen diffusion coefficient
$D_k^{(2)}$	$1.873 \cdot 10^{-5}$ m^2/s	knudsen diffusion coefficient
T_0	290 K	feed temperature
A	$1.9662 \cdot 10^{-3}$ m^2	bed cross sectional area
R	8.3145 J/(mol K)	universal gas constant
t_f	0.5 (-)	pressurization duration

B. Parameters for the Reverse Flow Reactor

The dimensionless parameters are given by

$$K_1 = \frac{t_f((1-\varepsilon)\lambda_s + u^2(\rho c_p)_g^2/(h a_v))}{L^2((\rho c_p)_s(1-\varepsilon) + (\rho c_p)_g \varepsilon)}$$

$$
\begin{aligned}
K_2 &= \frac{t_f u (\rho c_p)_g}{L((\rho c_p)_s(1-\varepsilon) + (\rho c_p)_g \varepsilon)} \\
K_3 &= \frac{\Delta T_{ad} t_f k_\infty e^{E_a/(RT_0)} (\rho c_p)_g}{T_0((\rho c_p)_s(1-\varepsilon) + (\rho c_p)_g \varepsilon)} \\
K_4 &= \frac{2U t_f}{r((\rho c_p)_s(1-\varepsilon) + (\rho c_p)_g \varepsilon)} \\
K_5 &= \frac{t_f D_{ax}}{L^2} \\
K_6 &= \frac{t_f u}{\varepsilon L} \\
K_7 &= \frac{t_f k_\infty e^{E_a/(RT_0)}}{\varepsilon} \\
g(\theta) &= \frac{a_v k_c e^{E_a(\theta-1)/(\theta R T_0)}}{a_v k_c + k_\infty e^{-E_a/(\theta R T_0)}}
\end{aligned}
$$

The values of the physical parameters are given in Table 9.

Table 9: The physical parameter values for the reverse flow reactor

D_{ax}	$4 \cdot 10^{-5}$ m^{2}s^{-1}	axial diffusion constant
t_f	60 s	flow reversal time
λ_s	1.26 W/(m K)	solid conductivity
L	1 m	reactor lenght
$(\rho c_p)_g$	624.4 J/(m^3 K)	volumetric heat capacity
$(\rho c_p)_s$	$1.319 \cdot 10^6$ J/(m^3 K)	volumetric heat capacity
u	2 m/s	superfical gas velocity
ΔT_{ad}	50 K	adiabatic temperature rise
ε	0.69 (-)	bed voidage
T_0	323 K	feed temperature
h	130 W/(m^2 K)	fluid/catalyst heat transfer coefficient
r	(varied) m	outer reactor radius
k_∞	$1.815 \cdot 10^7$ s^{-1}	frequency factor
E_a	1001.7 J/mol	activation energy
a_v	2628.8 m^{-1}	geometrical surface area of catalyst particles
k_c	0.115 m/s	mass transfer coefficient
R	8.3145 J/(mol K)	universal gas constant
U	(varied) W/(K m^2)	overall heat transfer coefficient

References

Croft, D. T. and Levan, M. G. (1994). Periodic states of adsorption cycles–I. Direct determination and stability. *Chemical Engineering Science.*, 49:1821–1829.

Jarausch, H. and Mackens, W. (1984). Numerical treatment of bifurcation branches by adaptive condensation. In Küpper, T., Mittelman, H., and Weber, H., editors, *Numerical Methods for Bifurcation Problems*, ISNM 70, pages 296–309. Birhäuser-Verlag.

Khinast, J., Gurumoorthy, A., and Luss, D. (1998). Complex dynamic features of a cooled reverse-flow reactor. *AIChE Journal*, 44:1128–1140.

Lust, K., Roose, D., Spence, A., and Champneys, A. R. (1998). An adaptive Newton-Picard algorithm with subspace iteration for computing periodic solutions. *SIAM Journal on Scientific Computing.*, 19:1188–1209.

Nilchan, S. and Pantelides, C. C. (1998). On the optimisation of periodic adsorption processes. *Adsorption.*, 4:113–147.

Saad, Y. (1992). *Numerical Methods for Large Eigenvalue Problems.* Algorithms and Architectures for Advanced Scientific Computing, Manchester University Press, Manchester.

Salinger, A. G. and Eigenberger, G. (1996). The direct calculation of periodic states of the reverse flow reactor–I. Methodology and propane combustion results. *Chemical Engineering Science.*, 51:4903–4913.

Shroff, G. and Keller, H. (1993). Stabilization of unstable procedures: The recursive projection method. *SIAM Journal on Numerical Analysis.*, 30:1099–1120.

Smith IV, O. J. and Westerberg, A. W. (1992). Acceleration of cyclic steady state convergence for pressure swing adsorption models. *Industrial and Engineering Chemistry Research.*, 31:1569–1573.

Van Noorden, T. L., Verduyn Lunel, S. M., and Bliek, A. (1999). Direct determination of cyclic steady states of cyclically operated packed bed reactors. In Keil, F., Mackens, W., Voss, H., and Werther, J., editors, *Volume 1: Molecular Properties, Reaction Diffusion Problems, Reaction Engineering, Simulation of Reactive Flows*, pages 311–318. International Workshop "Scientific Computing in Chemical Engineering II", Springer-Verlag.

Van Noorden, T. L., Verduyn Lunel, S. M., and Bliek, A. (2001). Acceleration of the determination of periodic states of cyclically operated reactors and separators. *submitted to Chemical Engineering Science.*